Multiple input multiple output dielectric resonator antenna with circular polarized adaptability for 5G applications

Multiple Input Multiple Output Dielectric Resonator Antenna with Circular Polarized adaptability for 5G Applications

S. S. Singhwal[a], B. K. Kanaujia[b], A. Singh[c], J. Kishor[d] and L. Matekovits[e]

[a]Department of Electronics and Communication Engineering, Uttarakhand Technical University, Dehradun, India.; [b]School of Computational and Integrative Science, Jawaharlal Nehru University, Delhi, India.; [c]Departement of Computer Science and Engineering, B.T.K. Institute of Technology, Dwarahat, Uttarakhand, India; [d]Department of Electronics and Communication Engineering, JIMS Engineering Management Technical Campus Greater Noida, India.; [e]Dipartimento di Elettronica e Telecomunicazioni, Politecnico di Torino, Torino, Italy

ARTICLE HISTORY
Compiled February 5, 2020

ABSTRACT
In this paper, the concept of circularly polarized agile, multiple-input multiple-output (MIMO) dielectric resonator antenna (DRA) structure for fifth generation (5G) new radio application in mobile terminal is presented. Two prototypes have been fabricated, namely one with cylindrical DRA (CDRA) referred as A1 and a second one with ring DRA (RDRA) named as A2. These practical realizations of dual-port MIMO antennas have been mounted on a Rogers 5870 substrate of octagonal shape with proper ground architecture. The proposed dual-port MIMO antennas have been excited with conformal probes and L-type feed network aiming to achieve circular polarization (CP). Measured impedance bandwidth (IBW) of A1 and A2 are 21.2% (3.15-3.9 GHz) and 22.2% (3.12-3.9 GHz), respectively. Moreover, for both antennas low mutual coupling between ports with minimum isolation of -20 dB over entire impedance bandwidth has been obtained by using triangular head slots in the ground plane. Measured axial ratio bandwidths (ARBW) in broadside direction ($\theta = 0$) are 5.66% (3.26-3.45 GHz) and 4.25% (3.45-3.6 GHz), respectively. Maximum gains are 7.3 dBi and 7.2 dBi, in that order. MIMO antenna parameters such as envelope correction coefficient (ECC), diversity gain (DG), mean effective gain (MEG) and total active reflection coefficient (TARC) are also calculated to verify MIMO performance parameters. The proposed antennas also demonstrate CP agility with insertion of concentric cylindrical shells of different radii.

KEYWORDS
Circular polarization; dielectric resonator antenna; multiple input multiple output; 5G.

1. Introduction

The fifth-generation (5G) wireless communication system can provide many advantages such as high capacity, higher data rate, and shorter latency. One of the promising 5G frequency band for wireless communication has been proposed around 3.5 GHz also known as Sub-6 GHz band and mid-band (1GHz-6GHz) [1–3]. This mid-band spec-

CONTACT L. Matekovits. Email: ladislau.matekovits@polito.it

trum will be more diverse and scarce, therefore capacity enhancement can be achieved by means of spectral efficiency. In order to meet these requirements multiple-input multiple-output (MIMO) technology has been deployed for 5G wireless operations. Applications of MIMO antenna in transmit/receive systems help passing through the previous limit of single antenna proposed by Claude Shannon [4,5]. MIMO antennas have now become synonymous to high-speed wireless communication technology such as long-term evolution (LTE), wireless local area network (WLAN), Worldwide Interoperability for Microwave Access (WiMAX) and 5G communications. MIMO technology improves channel capacity, link reliability in multipath propagation and assures higher transfer data rates in wireless communication [7–9]. Initially, MIMO antenna was proposed and implemented using microstrip patch antenna technology, until Ishmiya et al. [10,11] recommended solution making use of DRA for 802.11n applications. It paved the way for different DRA based MIMO designs.

It is observed that polarization diversity is often implemented by a dual-polarized antenna by employing linear polarizations (LP). From [10–26,35–40] all the DRA based MIMO antennas were LP examples. In comparison to LP antennas, CP antennas demonstrate several advantages such as effectiveness in combating multipath interference, robustness during polarization mismatching, etc. Due to these reasons, CP antennas constantly receive signal strength, which is very useful property in wireless communication where receiver antenna frequently changes its location in respect to the transmitter antenna [27]. DRA based CP MIMO antenna is recent area of research, so very few research articles [28–33] are published in this domain. Johnstone et al. presented an eight-port CDRA for MIMO system with different polarization states (LHCP, RHCP, and LP) [28]. However the different polarizations were achieved using various combinations of phased input at eight ports and isolation between ports was also refrained from discussion. Sahu et al. presented triple band MIMO DRA with gain 1.5 dBi, 4.2 dBi and 2.3 dBi but achieved CP only in one of the bands [29]. The same group also proposed a DRA based CP MIMO antenna for WLAN applications (5.2 GHz) [30]. Though, it suffered from low impedance bandwidth (simulated 10.28%) and minimum isolation of around -14 dB. In [31], two self complementary L-shaped DRAs were used in CP MIMO DRA. Here, isolation has been achieved by two self complementary slots cut in the ground plane. In [32], two cylindrical DRAs have been used in CP MIMO antenna using defected ground substrate (DGS) but measured ARBW is not reported. In [33], two rectangular DRAs have been used with optimised conformal patch structure to excite it and yielding a circularly polarized MIMO antenna. Isolation between elements is proposed using parasitic patch and diagonally positioned DRAs in [33]. In [34], two diagonal edge cut DRAs are excited by cross ring slot and EBG cell are used to enhance isolation. However, performance of this antenna is good but it suffer with design complexity. The literature review revealed the fact that research area of CP dielectric resonator based MIMO antenna is still in nurturing phase and lot of scope of improvement lie in this field.

This article proposes the concept of CP agility in DRA based MIMO antennas. Here, CP bandwidth can be controlled by inserting different cylindrical shells of different radii into the ring DRA. It is notable that minimum AR frequency has been varied comfortably without much variation in 10 dB impedance bandwidth. In particular, two dual-port DRA based CP agile MIMO antennas are proposed for 5G communications at 3.5 GHz. Major advantages of the discussed design are: (i) controllable CP; (ii) compactness in comparison to recent MIMO DRAs operating in same band; (iii) simple isolation mechanism and (iv) simple RDRA used instead of some complex structured DRA. The two prototypes have been fabricated and measured

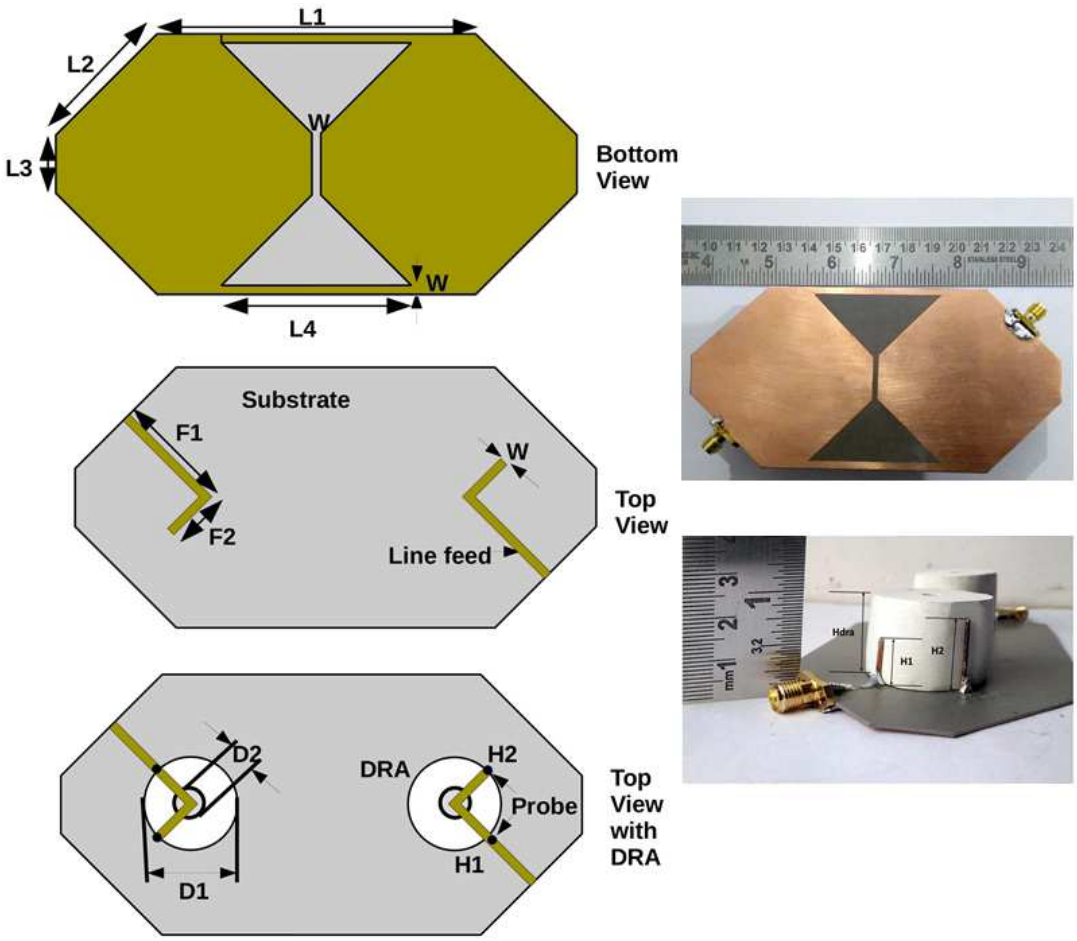

Figure 1.: Geometry of the Antenna

results have been compared with simulated data obtained from ANSYS' FEM-based high-frequency structural simulator (HFSS). Measured impedance bandwidth of A1 (with CDRA, for details see below) and A2 (with RDRA) are 21.2% (3.15-3.9 GHz) and 22.2% (3.12-3.9 GHz), respectively. The measured ARBW of A1 and A2 are 5.66% (3.26-3.45 GHz) and 4.25% (3.45-3.6 GHz) in broadside direction ($\theta = 0$). Isolation between ports is better than -20 dB over the entire impedance bandwidth and maximum gain of the A1 and A2 is 7.3 dBi and 7.2 dBi, respectively. MIMO performance metrics such as ECC, DG, MEG and TARC have also been measured and found well within acceptable limits. In particular, ECC is below 0.001, DG is above 9.99 dB MEG1 and MEG2 of both the ports have difference less than 3 dB and TARC is less than -20 dB for both the antennas.

2. Antenna Geometry and CP Agility

2.1. Geometry of the Antennas

Antenna design layout is shown in Fig. 1. It comprises a properly shaped ground plane hosting an octagonal substrate, two L type feed networks, conformal probes and

Table 1.: Design Parameters in mm

L1	85.5	L4	51	D1	25	H1	9	Height of DRA	18
L2	38.5	L5	35	D2	5	H2	15	Substrate thickness	0.8
L3	15.5	F1	31.2	F2	13.6	W	2.4		

two DRAs. All the design parameters, optimized using HFSS simulation software, are shown in Table 1.

RT Duroid with dielectric constant $\varepsilon_r = 2.33$, thickness 0.8 mm and $tan\delta = 0.0012$ has been used as substrate and Eccostock Hik bar with $\epsilon_r = 9.8$, $tan\delta = 0.001$ has been used as dielectric resonator antenna material. The height of the DRA is 18 mm. Each single DRA has been excited by two conformal probes having heights $H_1 = 9$ mm, $H_2 = 15$ mm and radius 1 mm as shown in Fig. 1. The conformal probe or patch excitation is an easy and effective feed method where it is required to couple field energy between DRA and feed line [41]. It also helps in matching by adjusting height of probe and excitation of $HE_{11\delta}$ mode. Conformal probe-1 excites $HE^{x}_{11\delta}$ and probe-2 excites $HE^{y}_{11\delta}$ mode in CDRA, as shown in Fig. 2. A CP field can be attained in a DRA by exciting two orthogonal components of fields with same magnitude and in phase quadrature. Probe-1 and probe-2, as shown in Fig. 1, have been placed on L-type feed network. Orthogonal modes inside DRA have been excited by these two probes. Phase quadrature relationship between both the orthogonal field components is controlled by optimizing the heights (H_1 and H_2) of the probes. Width of L-type microstrip feed line corresponds to 50 Ω characteristic impedance in no load condition is calculated and optimized using HFSS software. Design eq.(1) used in [6] for $HE_{11\delta}$ mode in CDRA have been used as first guess which is further optimized using HFSS software.

$$f_0 = \frac{c \times 6.324}{2\pi a\sqrt{\varepsilon_{rDRA}+2}}\left[0.27 + 0.36\frac{a}{2H} + 0.002\left(\frac{a}{2H}\right)^2\right] \quad (1)$$

where a, H and ε_{rDRA} are the radius, height, and dielectric constant of the DRA respectively, and c is the velocity of light in vacuum.

Table 2 displays different antennas with their respective S parameters. In antenna at s.no.1, a square substrate having dimension 110×110 mm^2 has been used. It showcased good impedance bandwidth of 22.8 % around 3.5 GHz but had two drawbacks which were large size of substrate (12100 mm^2) and poor isolation between ports with minimum isolation of -15 dB. Antenna at s.no.2 presented improvement in antenna-1 with reduced dimension of substrate i.e. 9356 mm^2 (77% of substrate area of antenna-1). To improve isolation between ports, antennas A1 and A2 have been designed. In A1 two CDRAs are placed on the substrate whereas in A2 two RDRAs are placed on the substrate. A comparison between simulated S-parameters of the two antennas is shown in Fig. 3. It is observed that there are two resonances due to dual-probe excitation. Isolation is achieved by introducing two triangular head slots cut in the ground plane with a linear slot at the middle of ground. Condition of the common ground which is essential for a MIMO antenna, attained by side slits on back of the substrate.

Table 2.: S-Parameters and ARBW of Different Stage Antennas

S.No.	Antenna	S-parameters	S_{11} (S_{22}) Bandwidth (GHz)	Min. Isolation S_{12} (S_{21}) dB	Axial Ratio Bandwidth (GHz)
1	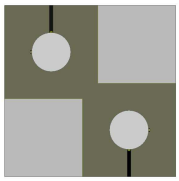	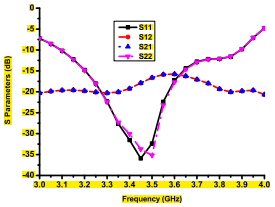	3.1-3.9 (22.8%)	-15	3.4-3.5 (100 MHz)
2	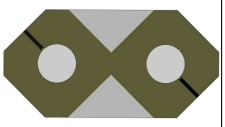	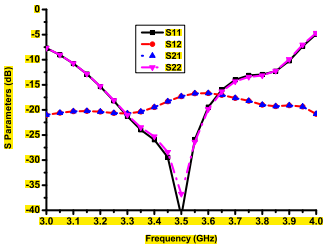	3.1-3.9 (22.8%)	-16.6	3.37-3.5 (130 MHz)
3	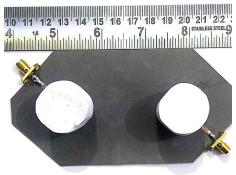	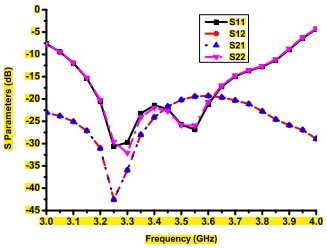	3.05-3.88 (23.95%)	-19.2	3.3-3.44 (140 MHz)
4	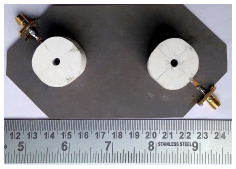	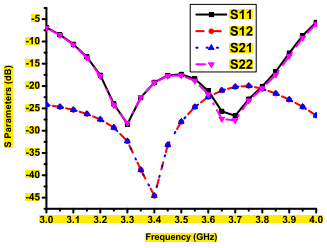	**3.08-3.94 (24.5%)**	**-20**	**3.42-3.57 (150 MHz)**

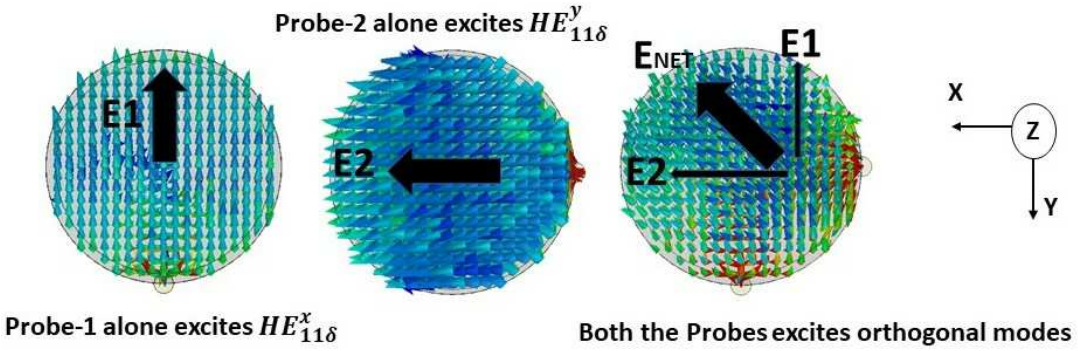

Figure 2.: Generation of fundamental orthogonal hybrid modes in cylindrical DRA

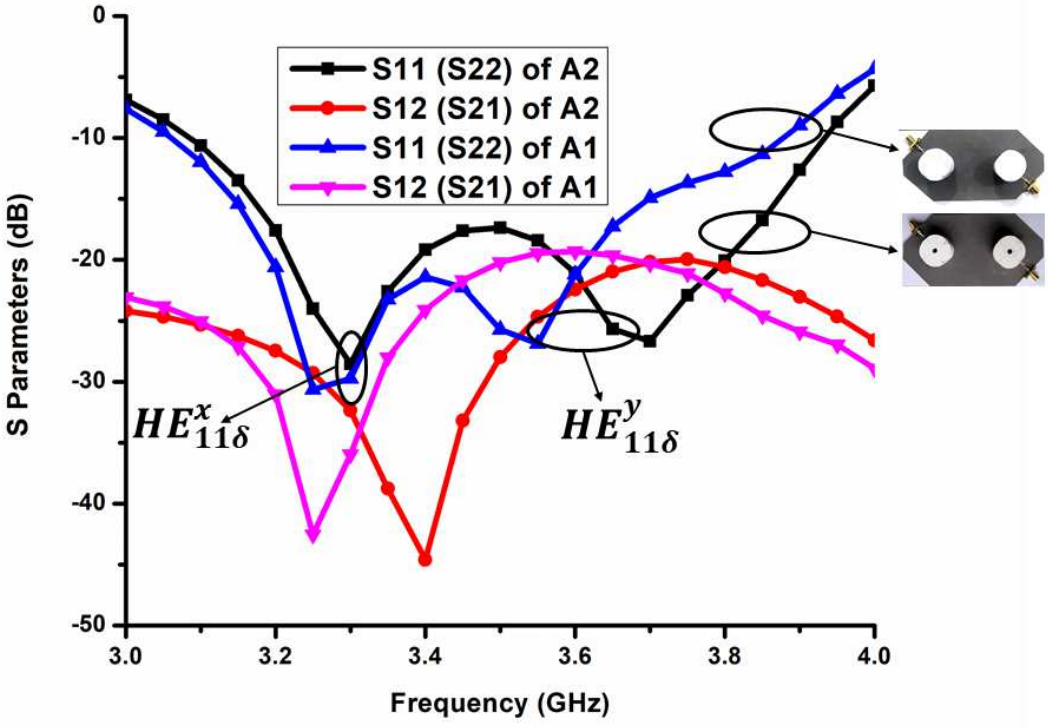

Figure 3.: Simulated S-parameters comparison of A1 and A2

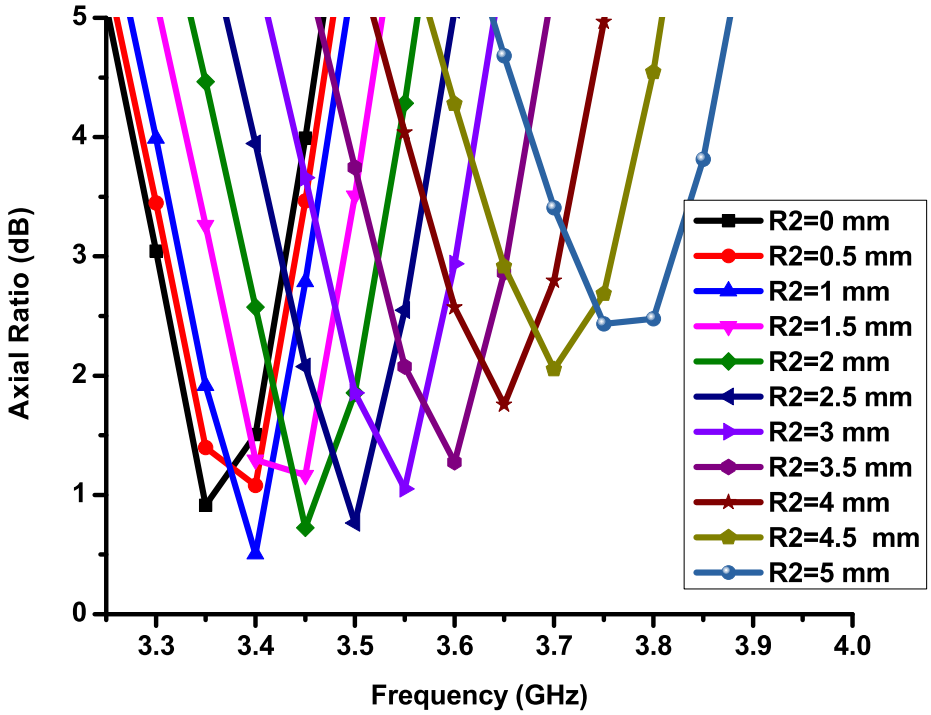

Figure 4.: Axial Ratio for different radii of inner shell of CDRA

2.2. CP Agility

CP agility describes the quickness of changing, minimum AR frequency by mechanical insertion/extraction of concentric cylindrical shells in/from the ring DRAs. Simulated ARs and S_{11} for different radii of inner shells, which are to be extracted from the CDRA, are shown in Fig. 4 and Fig. 5. These shows simulated ARs and S_{11} corresponding to radius $R2$=0 to 5 mm increased in step size of 0.5 mm. It is pertinent to note that minimum AR frequencies for different air gap cylinder radii, as shown in Fig. 4, are always in their respective 10 dB impedance bandwidths as shown in Fig. 5.

Fig. 6 shows five-concentric cylindrical shells to achieve CP agility. A1 can be configured when all the cylindrical shells are inserted in the ring DRA. Effect of gap between concentric cylindrical shells has also been studied and no significant consequences on the performance of antenna have been found, considering gap of 0.1-0.2 mm. Minimum AR frequency can easily be shifted by extracting cylindrical shells 1-5, in succession as shown in Fig. 6. In the literature, concept of movement of CP band with respect to inner vacuum cylinder diameter is not discussed especially in MIMO antennas where mutual operation of individual elements also affects its overall operation.

3. Results and Discussion

In this section, analysis of results and their implications are discussed. Two prototypes of dual-port circularly polarized MIMO DRA have been fabricated. Adhesive (glue) has been used to stick DRAs on substrate which resulted difference in measured and simulated results. Soldering deformity of connectors with ground and feed line might

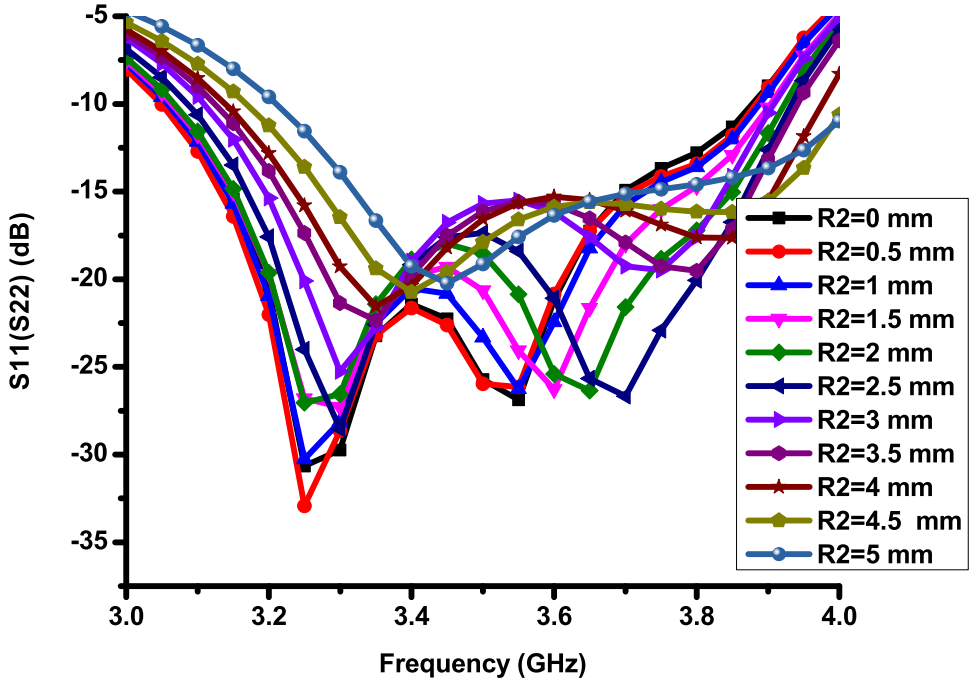

Figure 5.: S Parameters $S_{11}(S_{22})$ for different radii of inner shell of CDRA

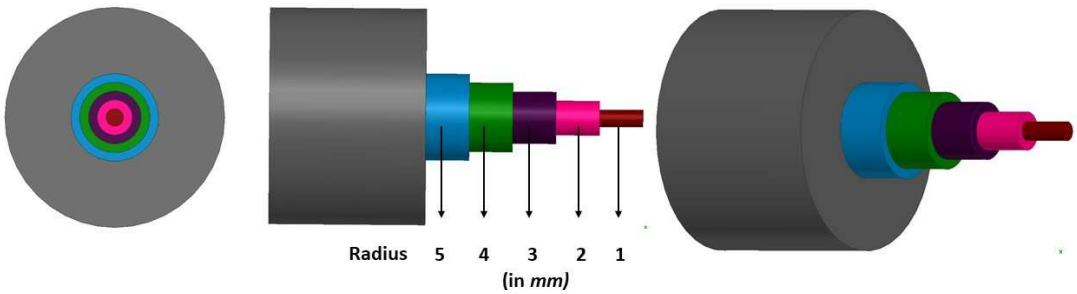

Figure 6.: Mechanical insertion and extraction of concentric cylindrical shells to achieve CP agility

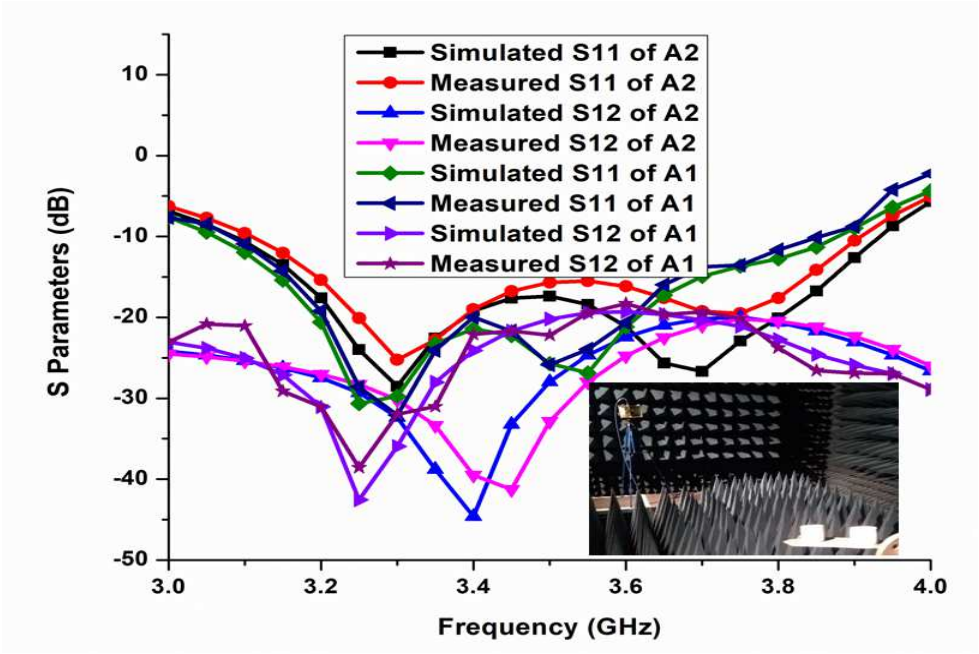

Figure 7.: Simulated and Measured S_{11} and S_{12} of A1 and A2

also be responsible for alteration of results. Far field results have been measured in anechoic chamber with corrugated horn antenna as reference antenna while keeping other port matched with 50 Ω. Standard measurement procedures [42–46] adopted for parameters measurement and eq.(2-8) have been implemented in MATLAB. Input radiation parameters to MATLAB have been provided by HFSS simulation software and measured radiation parameters of antenna, for simulated and measured values, respectively. A photograph of measurement setup is shown in the inset of Fig. 7.

Simulated and measured S-parameters of the antennas are shown in Fig. 7. Simulated and measured AR of the antennas are shown in Fig. 8. Simulated results are in good agreement with measured data. Measured impedance bandwidths of the antennas are 21.2% (3.15-3.9 GHz) and 22.2% (3.12-3.9 GHz), respectively. The measured 3 dB ARBWs are 190 MHz and 150 MHz in broadside direction. Port isolation is also greater than -20 dB over the complete impedance bandwidth and maximum gain of the antennas are 7.3 dBi and 7.2 dBi, respectively. ECC, DG, MEG and TARC have also been measured for both antennas. Figure 9 reports simulated and measured values of gain and radiation efficiency of the antennas. Measured radiation efficiency is greater than 90% for both the antennas whereas maximum gain 7.3 dBi and 7.2 dBi are obtained for the antennas, respectively. Figure 10 shows simulated and measured radiation field pattern (LHCP and RHCP) of A1 in E-Plane and H-Plane whereas Figure 11 shows the same for A2. Left hand CP component is greater than its right hand counterpart by more than acceptable limits for both the antennas. Radiation patterns have been plotted at minimum AR frequency for both the antennas.

To study and evaluate the MIMO or diversity performance of the proposed antenna ECC, DG, MEG and TARC have been analyzed. ECC is one of the main performance metric of MIMO system which describes isolation and correlation of communication channel with each other [9]. The DG identifies the amount of improvement that can be seen in MIMO in comparison to SISO (single input single output) system. In MIMO

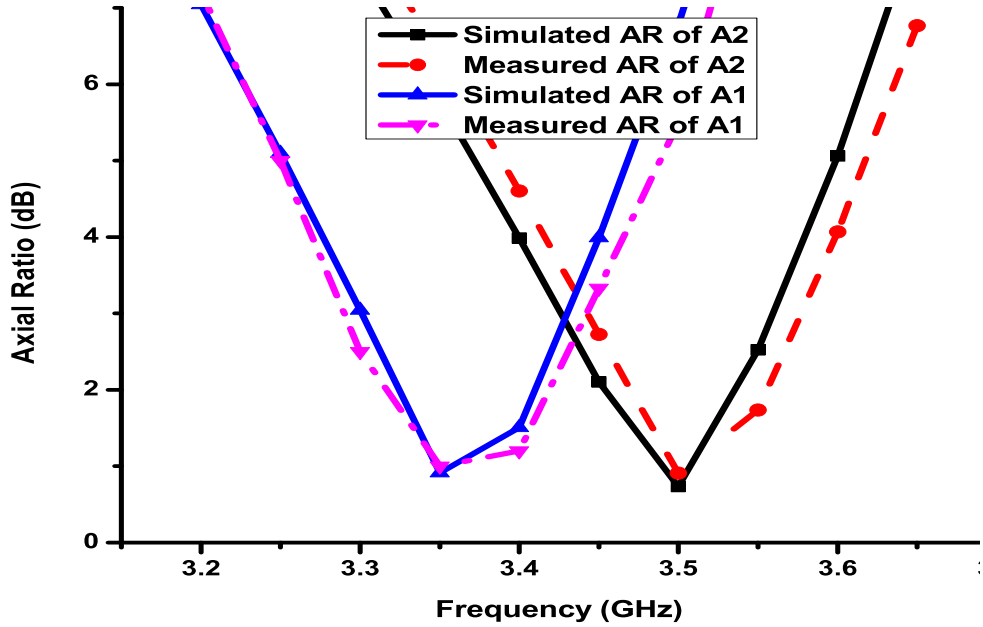

Figure 8.: Simulated and Measured Axial Ratio of A1 and A2

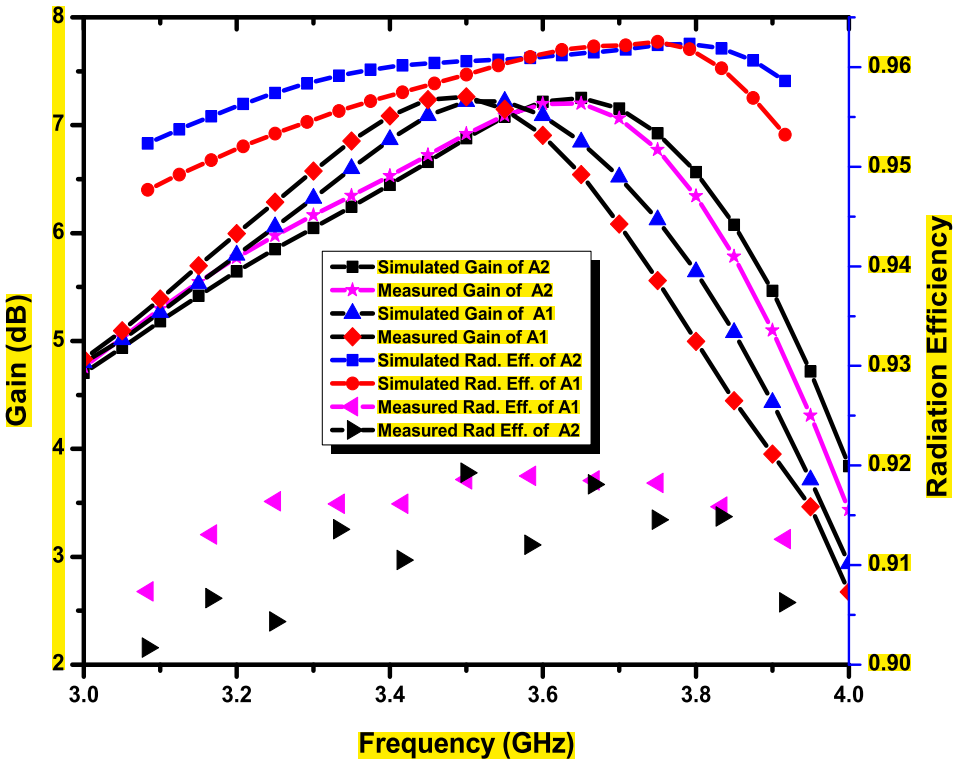

Figure 9.: Gain (Measured and Simulated) and Radiation Efficiency (Measured and Simulated) of A1 and A2

systems, the adjacent radiators when operating simultaneously can influence the performance of each other. This parameter is described by TARC. MEG measures the amount of power received by the MIMO antenna in comparison to a standard antenna in the standard environment. For a good diversity performance of MIMO antenna, difference between MEG1 and MEG2 should be less than 3 dB [35]. ECC, DG and TARC have been calculated using eq. (2), eq. (3), and eq. (8) respectively, given in [9,47,48] where as MEG is calculated by eq. (4) given in [35]. Simulated and measured ECC has been obtained less than 0.001 which satisfies the limit ECC<0.3 mentioned in [9] for MIMO system. DG is also approximately 10 dB over entire bandwidth which is desired for MIMO system [9]. Desirable value of TARC for a MIMO system is less than 0 dB.

$$ECC = \frac{\left| \iint_{4\pi} \left[\overrightarrow{F_1}(\theta,\phi) * \overrightarrow{F_2}(\theta,\phi) \right] d\Omega \right|^2}{\iint_{4\pi} \left| \overrightarrow{F_1}(\theta,\phi) \right|^2 d\Omega \iint_{4\pi} \left| \overrightarrow{F_2}(\theta,\phi) \right|^2 d\Omega} \tag{2}$$

where $\overrightarrow{F_i}(\theta,\phi)$ is three dimensional field radiation pattern of MIMO antenna when port-i is excited. Ω is solid angle and * represents the Hermitian product operator.

$$DG = 10\sqrt{1 - ECC^2} \tag{3}$$

$$MEG_i = 0.5\left[1 - \sum_{j=1}^{N} |S_{ij}|^2\right] \tag{4}$$

For two port MIMO antenna eq. (4) is expanded in eq. (5) and eq. (6), whereas eq. (7) represents the condition of difference between two MEGs should be less than 3 dB.

$$MEG_1 = 0.5\left[1 - |S_{11}|^2 - |S_{12}|^2\right] \tag{5}$$

$$MEG_2 = 0.5\left[1 - |S_{21}|^2 - |S_{22}|^2\right] \tag{6}$$

$$| MEG_1 - MEG_2 | < 3 \text{ dB} \tag{7}$$

$$TARC = \sqrt{\frac{\left(S_{11} + S_{12}e^{j\theta}\right)^2 + \left(S_{21} + S_{22}e^{j\theta}\right)^2}{2}} \tag{8}$$

where θ is input feeding phase.

Table 3 summarizes the MIMO performance metrics results of A1 and A2 at 3.35 GHz and 3.5 GHz, respectively. Figure 12 shows photographs of fabricated antennas, A1 with CDRA and A2 with two diameters of internal vacuum cylinder. Initially A2 with diameter D_2=2.5 mm is fabricated and its results has been measured then measurement process was repeated after drilling the diameter D_2=5 mm. Measured

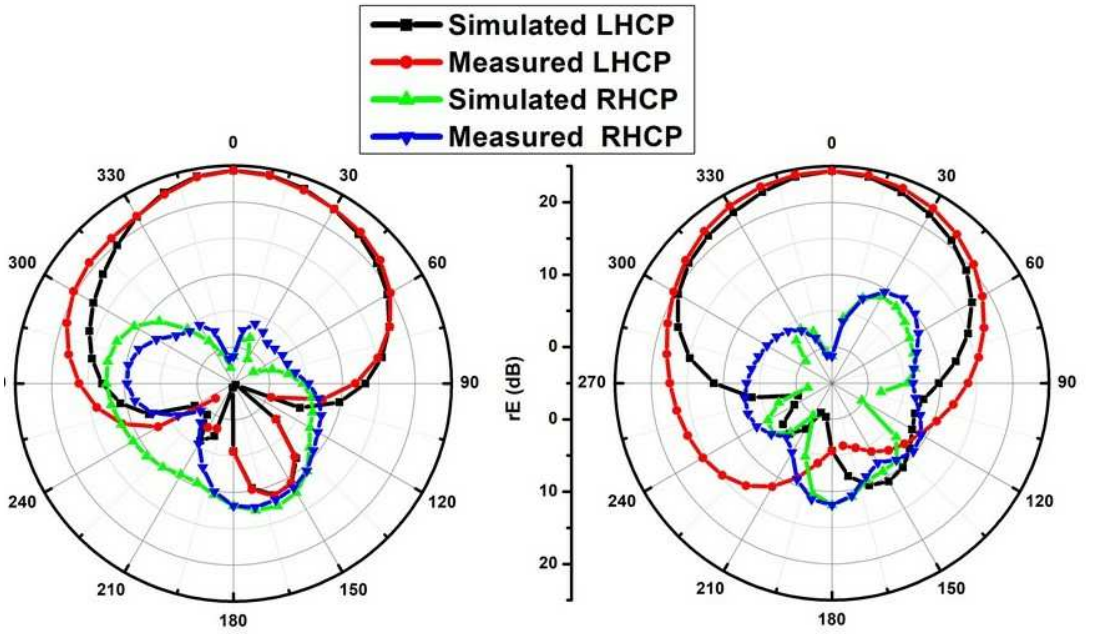

Figure 10.: Measured and simulated E-plane (left) and H-Plane (right) radiation pattern of A1 at 3.35 GHz

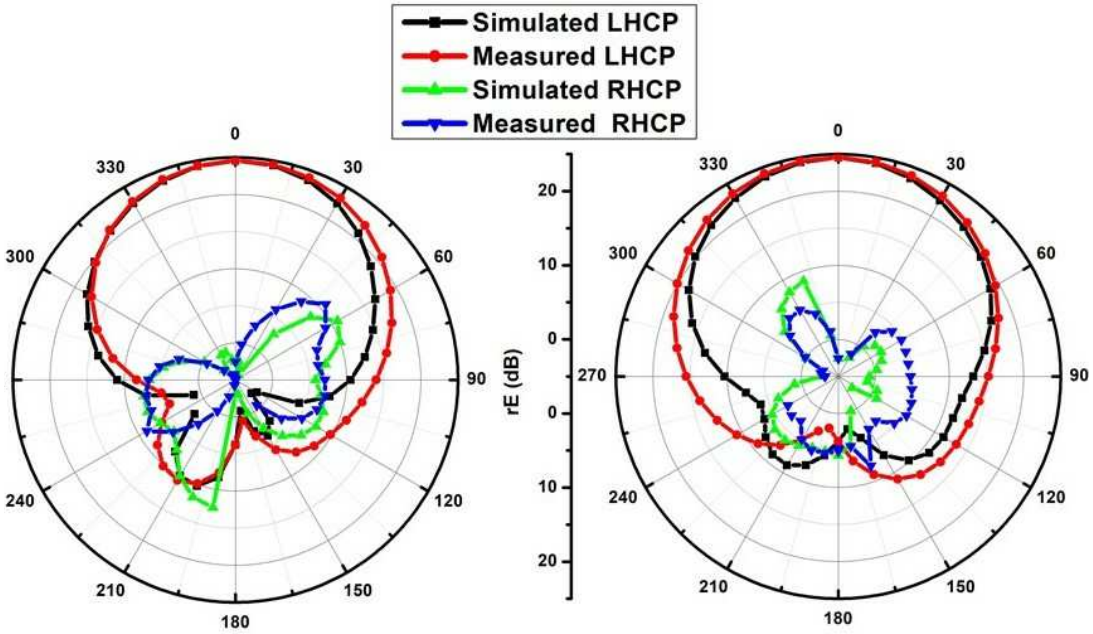

Figure 11.: Measured and simulated E-plane (left) and H-Plane (right) radiation pattern of A2 at 3.5 GHz

Table 3.: MIMO parameters of A1 and A2

	ECC	DG	MEG1	MEG2	TARC
Simulated (A1 at 3.35 GHz)	1.3×10^{-4}	9.99	−13.98	−13.88	−44.98
Measured (A1 at 3.35 GHz)	2.7×10^{-5}	9.99	−13.8	−13.5	−43.2
Simulated (A2 at 3.5 GHz)	1.2×10^{-4}	9.99	−14.2	−14.1	−35.02
Measured (A2 at 3.5 GHz)	5.4×10^{-5}	9.99	−14.4	−14.3	−34.5

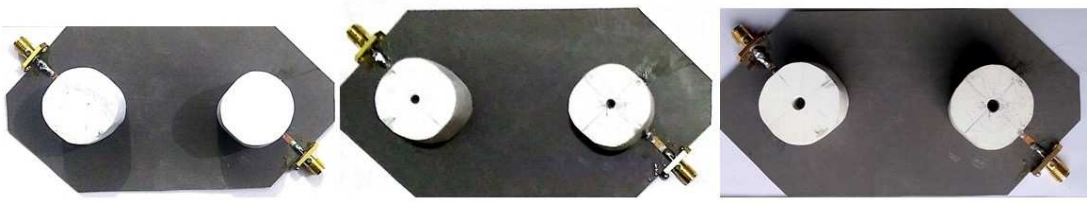

Figure 12.: Structures of Fabricated Antennas with different diameters of internal vacuum cylinder in CDRA (a) D_2=0 mm, (b) D_2=2.5 mm (c) D_2=5 mm. (left to right)

results of all three cases have been found in agreement with simulated results hence concept of CP agility has been verified. Measured results of diameter D_2=2.5 mm of Fig. 12 are not shown for brevity. Table 4 shows the comparison of proposed MIMO DRA with other recently published MIMO DRA that includes circularly polarized and linearly polarized radiators. In this Table 4 Circularly Polarized MIMO DRA are from [29–34]. Proposed MIMO DRA has comparable output parameters as that of Chen et.al. [34]. But major advantage of proposed antenna in comparison to [34] are 1) simple ring DRAs instead of uneven cut DRA 2) Simple isolation mechanism in place of complex EBG structure 3) Compact in size with lesser surface area of substrate.

4. Conclusions

In this paper, a concept of CP agility is presented with two antennas operating in Sub-6 GHz band. Two dual-port multiple input multiple output DRAs are proposed. Antennas are fabricated on Rogers RT Duroid substrate having dielectric constant 2.33 and thickness 0.8 mm. Two fabricated antennas exhibit good impedance bandwidth of 21.2% and 22.2% and low mutual coupling between ports with minimum isolation of -20 dB. These antennas also exhibit circular polarization with axial ratio bandwidth of 190 MHz and 150 MHz. Diversity performance is also analyzed and entire analysis confirms that proposed MIMO antennas can be a good candidate for 5G communications in Sub-6 GHz band.

Table 4.: Comparison of Proposed Antenna with other published MIMO DRA

Ref.	Impedance Bandwidth (GHz)	ARBW (GHz)	Gain (dBi)	Isolation (dB)
23	5.4-6.0	-	5	-18
24	3.4-8.2	-	3	-20
25	3.4-3.7, 5.15-5.35	-	5.7, 6.61	-13
28	3.42-3.8, 4.97-5.5	-	5.2. 6.38	-20
29	2.21-3.13, 3.4-3.92, 5.3-6.1	5.62-5.82	1.5, 4.1, 2.3	-20
30	4.89-5.42	5.16-5.38	5	-12
31	5.2-6.08	5.2-5.58	4	-19
32	5.25-6.25	not given	4.7	-25
33	3.5-4.95	3.58-4.4	6.2	-28
34	3.15-3.93	3.3-3.8 (simulated)	7.4 (Simulated)	-24
35	4.7-6.2	-	7.4	-15
36	5.27-5.65	-	5.99	-22
37	3.4-3.7 , 5.15-5.35	-	5.6	-46
38	5.6-5.9	-	4.8	-20
39	1 GHz bandwidth around 30 GHz	-	6.9, 7.6	-27
40	3.24-6.0	-	7.45	-20
Proposed-A1	**3.12-3.9**	**3.26-3.45 (190 MHz)**	**7.3**	**-20**
Proposed-A2	**3.15-3.9**	**3.43-3.58 (150 MHz)**	**7.2**	**-20**

Acknowledgement

Binod K. Kanaujia acknowledges DBT & COE project funds for providing infrastructure support and DST-PURSE, Govt. of India & UPE II ID:340, JNU for providing support throughout this work. Authors would also like to acknowledge the Principal, G.B. Pant Engineering College Delhi, India, for providing antenna measurement facility at G.B.P.C.E. Delhi.

References

[1] "Statement: Improving Consumer Access to Mobile Services at 3.6 GHz to 3.8 GHz. Accessed: Oct. 24, 2018." [Online]. Available: https:// www. ofcom. org. uk/ consultations-and-statements/category-1/future-use-at-3.6-3.8-ghz.

[2] "Spectrum for 4G and 5G" Accessed: Oct. 24, 2018. [Online]. Available: https://www.qualcomm.com/media/documents/files/spectrum-for-4g-and-5g.pdf

[3] Ren Z., Wu S., Zhao A., "Coexist design of sub-6 GHz and millimeterwave antennas for 5G mobile terminals," in Proc. Int. Symp. Antennas Propag., Busan, South Korea, 2018, pp. 805–806.

[4] Shannon, C.E., "A mathematical theory of communication," Bell Syst. Tech. J., vol. 27,

pp. 623–656, 1948.
[5] Allen B., Malik W.Q., Smith P.J., et al, "Demystifying MIMO," IET Commun. Eng., vol. 4 , no. 6, pp. 38–42, 2006.
[6] Mongia R.K. and Bhartia P., "Dielectric resonator antennas—A review and general design relations for resonant frequency and bandwidth,"Int. J. RF Microw Millim. Comput.-Aided Eng., vol.4 , no. 3, pp. 230–247, 1994.
[7] Karaboikis, M.P., Papamichael, V.C., Tsachtsiris, G.F., et al., "Integrating compact printed antennas onto small diversity/MIMO terminals," IEEE Trans. Antennas Propag., vol. 56, no. 7, pp. 2067–2078, 2008.
[8] Konanur, A.S., Gosalia, K., Krishnamurthy, S.H., et al., "Increasing wireless channel capacity through MIMO systems employing co-located antennas," IEEE Trans. Microw. Theory Tech., vol. 53, no. 6, pp. 1837–1844, 2005.
[9] Sharawi, M.S, "Printed multi-band MIMO antenna systems and their performance metrics," IEEE Antennas Propag. Mag., vol. 55, no. 5, pp. 218–232, 2008.
[10] Ishimiya, K., Langbacka, J., Ying, Z., et al., "A compact MIMO DRA antenna," IEEE Int. Workshop on Antenna Technology: Small Antennas and Novel Metamaterials, Chiba, Japan, pp. 286–289, 2008.
[11] Ishimiya, K., Ying, Z., Langbacka, J., "A compact MIMO DRA for 802.11n application," IEEE Antennas and Propagation Society Int. Symp. CA, July 2008.
[12] Yan, J.B., Bernhard, J.T., "Design of a MIMO dielectric resonator antenna for LTE femtocell base stations," IEEE trans. Antennas Propag., vol. 60, pp. 438-444, 2012.
[13] Thamae, L.Z., Wu, Z., "Dielectric resonator based multiple-input-multiple-output antennas and channel characteristic analysis," IET Microw. Antennas Propag, vol. 6, no. 9, pp. 1084–1089, 2012.
[14] Yan, J.B., Bernhard, J.T, "Implementation of a frequency agile MIMO dielectric resonator antenna," IEEE Trans. Antennas Propag., vol. 61 , no. 7, pp. 3434–3441, 2013.
[15] Roslan, S.F., Kamarudin, M.R., Khalily, M., et al, "An MIMO rectangular dielectric resonator antenna for 4G applications," IEEE Antennas Wirel. Propag. Lett., no. 13, pp. 321–324, 2014.
[16] Sharawi, M.S., Podilchack, S.K., Antar, Y.M.M, "A low profile dual-band DRA-based MIMO antenna system for wireless access points," IEEE Int. Symp. on Antennas and Propagation and USNC/URSI National Radio Science Meeting, Vancouver, BC, pp. 707–708, 2015.
[17] Hussain, M.T., Hammi, O., Sharawi, M.S., et al, "A dielectric resonator based millimeter-wave MIMO antenna array for hand-held devices," IEEE Int. Symp. on Antennas and Propagation and USNC/URSI National Radio Science Meeting, Vancouver, BC, pp. 3–4, 2015.
[18] Roslan, S.F., Kamarudin, M.R., Khalily, M., et al, "An MIMO F-shaped dielectric resonator antenna for 4G applications," Microw. Opt. Technol. Lett., vol. 57 , no. 12, pp. 2931–2936000, 2015.
[19] Hussain, M.T., Sharawi, M.S., Podilchack, S.K., et al, "Closely packed millimeter-wave MIMO antenna arrays with dielectric resonator elements," *1*0th European Conf. on Antennas and Propagation (EuCAP), Davos, pp. 1–4, 2016.
[20] Nasir, J., Jamaluddin, M.H., Khalily, M., et al, "Design of an MIMO dielectric resonator antenna for 4G aplications," Wirel. Pers. Commun., vol. 88 , pp. 525–536, 2016.
[21] Sharma A., Biswas A.,"Wideband multiple-input–multiple-output dielectric resonator antenna," IET Microw. Antennas Propag., vol. 11, no. 4, pp. 496–502, 2017.
[22] Sharma A., Das G., Gangwar R.K., "Design and analysis of tri-band dual-port dielectric resonator based hybrid antenna for WLAN/WiMAX applications," Electronic Letters, vol. 12, no. 6, pp. 986–992, 2018.
[23] Das G., Sharma A., Gangwar R.K , Sharawi M.S., "Compact back-to-back DRA-based four-port MIMO antenna system with bi-directional diversity," Electronic Letters, vol. 54, no. 14, pp. 884–886, 2018.
[24] Das G., Sharma A., Gangwar R. K., ""Wideband self-complementary hybrid ring dielec-

tric resonator antenna for MIMO applications," IET Microwaves, Antennas and Propagation, Vol.12 , Issue.1, 2018.
[25] Khan A. A., Jamaluddin M. H., Aqeel S., Nasir J., Kazim J. R., Owais O. "Dual-band MIMO dielectric resonator antenna for WiMAX/WLAN applications" IET Microwaves, Antennas and Propagation, Vol.11, No. 1,2017.
[26] Khan A.A., Jamaluddin M.H., Nasir J., Khan R., Aqeel S., Saleem J., Owais O., "Design of a Dual-Band MIMO Dielectric Resonator Antenna with Pattern Diversity for WiMAX and WLAN applications" Progress In Electromagnetics Research M, Vol. 50, 65–73, 2016
[27] Dicandia F.A., Genovesi S., and Monorchio A., "Analysis of the performance enhancement of MIMO systems employing circular polarization," IEEE Trans. On Antenna and Propag., , vol. 65, pp. 4824–4835, 2015.
[28] Johnstone, J.C., Podilchak, S.K., Clénet, M., et al., "A compact cylindrical dielectric resonator antenna for MIMO applications," IEEE Antennas and Propagation Society Int. Symp. (APSURSI),Memphis, TN, pp. 1938–1939, 2014.
[29] Sahu N.K., Das G. and Gangwar R.K., "Dual polarized triple-band dielectric resonator based hybrid MIMO antenna for WLAN/WiMAX applications" Microw Opt Technol Lett, vol. 60, pp-1033-1041, 2018.
[30] Sahu N.K., Gangwar R.K., Kumari P., "Dielectric Resonator Based Circularly Polarized MIMO Antenna for WLAN Applications," International Conference on Microwave and Photonics (ICMAP 2018), 2018.
[31] Sahu N.K., Das G., Gangwar R.K."L-shaped dielectric resonator based circularly polarized multi-input-multi-output (MIMO) antenna for wireless local area network (WLAN) applications" Int J RF Microw Comput Aided Eng. 2018.
[32] Das G., Sharma A., Gangwar R.K "Dielectric resonator based circularly polarized MIMO antenna with polarization diversity,"Microw. Opt.Technol.Lett. vol. 60, pp. 685–693, 2018.
[33] Iqbal J., Illahi U., Sulaiman M.I., Alam M., Mazliham M. S., Yasin M. N "Mutual Coupling Reduction Using Hybrid Technique in Wideband Circularly Polarized MIMO Antenna for WiMAX Applications,"IEEE Access vol. 7, pp. 40951 - 40958, 2019.
[34] Chen H. N., Song J., Park J. , "A Compact Circularly Polarized MIMO Dielectric Resonator Antenna Over Electromagnetic Band-Gap Surface for 5G Applications," *IEEE Access*, pp. 1408889-140898, Sep. 2019.
[35] Singhwal S. S., Kanaujia B.K., Singh A., Kishor J. , "Dual-port MIMO dielectric resonator antenna for WLAN applications," *Int J RF Microw Comput Aided Eng.*, 2019;e22108.
[36] Sharma A., Sarkar A., Biswas A., Akhtar M.J., "Equilateral Triangular Dielectric Resonator based Co-Radiator MIMO Antennas with Dual Polarization," *IET Microwaves, Antennas and Propagation*, pp. 2161-2166, 2018.
[37] Khan, AA, Khan, R, Aqeel, S, Nasir, J, Saleem, J, Owais, J., "Design of a dual-band MIMO dielectric resonator antenna with high port isolation for WiMAX and WLAN applications," *Int J RF Microw Comput Aided Eng.*, 2017.e21058.
[38] Das G., Sahu N. K., Sharma A., Gangwar R. K., Sharawi M. S., "Dielectric resonator-based four-element eight-port MIMO antenna with multi-directional pattern diversity," *IET Microwaves, Antennas and Propagation*, vol. 13, no. 1, pp. 16-22, 9 1 2019.
[39] Sharawi M. S., Podilchak S. K., Hussain M.T., Antar Y. M. M., "Dielectric resonator based MIMO antenna system enabling millimetre-wave mobile devices," *IET Microwaves, Antennas and Propagation*, vol. 11, no. 2, pp. 287-293, 29 1 2017.
[40] Sharma A., Sarkar A., Biswas A., "A-shaped wideband dielectric resonator antenna for wireless communication systems and its MIMO implementation," *Int J RF Microw Comput Aided Eng.*, e21402 2018.
[41] Chowdhury R., Mishra N.,Sani M.M. and Chaudhary R.K., "Analysis of a Wideband Circularly Polarized Cylindrical Dielectric Resonator Antenna With Broadside Radiation Coupled With Simple Microstrip Feeding," IEEE Access, vol. 5, pp. 19478-19485, 2017.
[42] Elshirkasi A.M., Al-Hadi A.A., Mansor M.F.,Khan R., Soh P.J., "Envelope Correlation Coefficient of a Two-Port MIMO Terminal Antenna under Uniform and Gaussian Angular Power Spectrum with User's Hand Effect", *Progress In Electromagnetics Research C*, Vol.

92, 123–136, 2019.

[43] Orlenius C., Andersson M., "Repeatable Performance Measurements of MIMO Systems in Connected Reverberation Chambers with Controlled Keyhole Effect", *RadioEngineering* Vol. 18, No. 4, Dec 2009.

[44] Federal Communications Commission,"Emissions Testing of Transmitters with Multiple Outputs in the Same Band", Oct.31, 2013.

[45] IEEE Standard Test Procedures for Antennas, 1979. DOI : $10.1109/IEEESTD.1979.120310$

[46] Sarrazin F., Pflaum S., Delaveaud C.,"Radiation efficiency measurement of a balanced miniature IFA-inspired circular antenna using a differential Wheeler cap setup" *International Workshop on Antenna Technology (IWAT 2016)*, Feb 2016, Cocoa Beach, FL, United States. pp.64, IWAT, 2016.

[47] Sharawi, M.S,"Current Misuses and Future Prospects for Printed Multiple-Input, Multiple-Output Antenna Systems [Wireless Corner]," *IEEE Antennas and Propagation Magazine*, vol. 59, no. 2, pp. 162-170, April 2017

[48] Sharawi, M.S.,"Advancements in MIMO antenna systems" Chapter-4 published by IET Nov. 2018. In the book "Developments in Antenna Analysis and Synthesis", Edited by Raj Mittra.